Preparation of thin-film electrolyte from chitosan-containing ionic liquid for application to electric double-layer capacitors

Ditpon Kotatha, Yoshiki Torii, Keito Shinomiya, Mayuko Ogino, Satoshi Uchida, Masashi Ishikawa, Tetsuya Furuike, Hiroshi Tamura

PII: S0141-8130(18)35236-X
DOI: https://doi.org/10.1016/j.ijbiomac.2018.12.006
Reference: BIOMAC 11165

To appear in: *International Journal of Biological Macromolecules*

Received date: 1 October 2018
Revised date: 16 November 2018
Accepted date: 1 December 2018

Please cite this article as: Ditpon Kotatha, Yoshiki Torii, Keito Shinomiya, Mayuko Ogino, Satoshi Uchida, Masashi Ishikawa, Tetsuya Furuike, Hiroshi Tamura , Preparation of thin-film electrolyte from chitosan-containing ionic liquid for application to electric double-layer capacitors. Biomac (2018), https://doi.org/10.1016/j.ijbiomac.2018.12.006

Preparation of Thin-film Electrolyte from Chitosan-Containing Ionic Liquid for Application to Electric Double-layer Capacitors

Ditpon Kotatha, Yoshiki Torii, Keito Shinomiya, Mayuko Ogino, Satoshi Uchida, Masashi Ishikawa, Tetsuya Furuike, Hiroshi Tamura*

Faculty of Chemistry, Materials and Bioengineering, Kansai University, Osaka 564-8680, Japan

*Corresponding author: tamura@kansai-u.ac.jp

Abstract

A novel thin-film electrolyte (TFE) based on chitosan (CS) with 1-ethyl-3-methylimidazolium tetrafluoroborate ($EMImBF_4$) was prepared by a new procedure for use as a solid electrolyte in electric double-layer capacitors (EDLCs). In this system, $EMImBF_4$ plays important roles as both a dissolving solution and a charge carrier for EDLC application. By analyzing and characterizing the obtained products, the CS-TFEs showed a surface without CS/$EMImBF_4$ phase separation and with high thermal stability and good tensile properties. The electrochemical properties were measured as the charge–discharge performance, the discharge capacitance, and alternating-current impedance. A test cell with CS-TFE with a calculated dry thin-film content of 80 wt% $EMImBF_4$ showed a comparable *IR* drop and higher discharge capacitance than a liquid-phase $EMImBF_4$ system and also showed low electrode/electrolyte interfacial resistance. Consequently, this novel CS-TFE is suitable for high-performance EDLCs and improves the safety of such devices.

Highlights

- A new method for preparing a chitosan thin-film electrolyte (CS-TFE).
- 1-ethyl-3-methylimidazolium tetrafluoroborate ($EMImBF_4$) used for this preparation.
- $EMImBF_4$ is a solvent and charge carrier for electric double-layer capacitors (EDLC).
- The obtained CS-TFEs have a homogeneous surface, are tensile, and thermally stable.
- The obtained CS-TFE can have high-performance and be safety-oriented EDLCs.

Keywords: Chitosan, Solid electrolyte, Thin-film electrolyte, Ionic liquid, Electric double-layer capacitors

1. Introduction

Electric double-layer capacitors (EDLCs), also known as super capacitors or ultracapacitors, are electrochemical devices that have received much attention in recent years because of their outstanding properties of long cycle lifetime and high sustained power density [1–3]. Likewise, electrolytes based on natural polymers have been developed vigorously for electric devices because of their biodegradation properties, low cost, non-toxicity, environmental friendliness, richness in nature, and capacity to satisfy sustainable biopolymer development. Many natural polymers have been used as polymer electrolytes, such as alginate [4–6], carrageen [7, 8], agar [9, 10], starch [11–13], natural rubber [14, 15], pectin [16], cellulose [17], and chitosan (CS) [18–20], the last of which is one of the most abundant biomaterials.

CS is a cationic biopolymer obtained from either fully or partially deacetylated chitin. As a natural polymer, CS is a copolymer of D-glucosamine and *N*-acetyl-D-glucosamine connected via β (1-4) linkage and is present in crustacean shells, insect exoskeletons, and cell walls of some fungi [21–26]. CS is often identified by its degree of deacetylation (DDA), namely, the ratio of D-glucosamine to *N*-acetyl-D-glucosamine. The DDA is typically in the range of 70%–100% and relates to CS properties such as its surface energy, crystallinity and degradation [27, 28]. Because of its excellent biodegradability, biocompatibility, hemostasis, and antimicrobial activity and the fact that it is easily processed into various forms (e.g., hydrogels, membranes, scaffolds, beads, sponges, nanofibers, and nanoparticles), CS is extremely valuable for

biomedical and pharmaceutical applications [29]. Furthermore, many studies have reported that CS is a promising electrolyte for EDLCs in terms of giving their high operating performance [30–33].

Often referred to as green solvents [34–36], ionic liquids (ILs) are organic salts whose melting points are near room temperature. One such IL is 1-ethyl-3-methylimidazolium tetrafluoroborate ($EMImBF_4$). With its high ionic conductivity and low viscosity, $EMImBF_4$ is widely used as an electrolyte in EDLCs [37–42]. In addition, ILs exhibit unique physicochemical properties such as near-zero vapor pressure, high chemical and thermal stabilities, and the facts that they remain liquid over a broad temperature range and are good at dissolving a variety of organic and inorganic compounds [34–36]. As such, ILs have been studied recently for their abilities to dissolve native polysaccharides and some natural materials [35, 36, 43–48] including CS [49–55].

Previously, Yamagata et al. [30, 31] prepared gel electrolytes from CS including ILs via hydrogel preparation methods for use in EDLCs. Although the method provided gel electrolytes with high performance despite the use of gel electrolytes, it adversely resulted in low tensile strength, which is a favorable property for solid-electrolytes to be used in EDLCs. This failed to approximately control the IL content in the obtained sample. Thus, development on a novel method to overcome these disadvantages is desirable.

The aim of the present study is to propose a new method to provide an IL-based thin-film

electrolyte (TFE) with relatively high tensile property and appropriate IL-content. In addition, the novel CS-TEFs were used as a solid electrolyte for EDLCs to improve their safety and performance. To the best of our knowledge, this study is the first report on preparation of TFEs by using CS dissolved in the mixture of $EMImBF_4$ and water (see CS and $EMImBF_4$ structure in Fig. 1). $EMImBF_4$ in this system plays important roles as both a dissolving solution and a charge carrier for EDLC due to high ionic conductivity and low viscosity. The obtained TFE is characterized, and the electrochemical properties of an EDLC test cell containing the electrolyte were assessed.

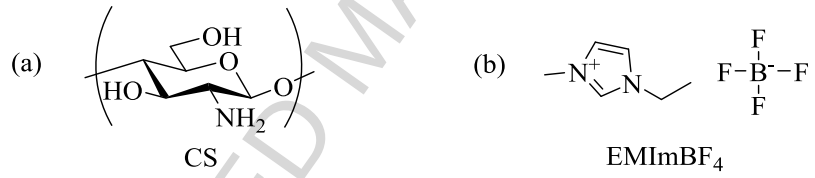

Fig. 1. Structure of (a) CS and (b) $EMImBF_4$.

2. Materials and methods

2.1. Materials

Chitosan (CS; FM-80, DDA 88.3%, Viscosity 30 mPa S, Mw 24.8×10^4) was supplied by Koyo Chemical Company (Japan), and 1-ethyl-3-methylimidazolium tetrafluoroborate ($EMImBF_4$, 99.0%) was purchased from Toyo Gosei Company (Japan). The number average molecular weight (Mw) of CS was re-measured by gel permeation chromatography (GPC) method.

2.2. Preparation of chitosan thin-film electrolyte

CS powder was dispersed in a mixture of $EMImBF_4$ and deionized (DI) water in a glass bottle with different stoichiometric ratios as listed in Table 1, and the calculated $EMImBF_4$ in dry film was calculated according to Eq. (1). The mixture was stirred at 40°C for four days and then left at room temperature for 10 days. The obtained solution was cast into a frame made with a glass supporter (thickness; 1200-μm) on a Teflon sheet and was soaked in methanol for 3 min. The CS-TFE was then dried at 25°C (room temperature) for 24 h, then the dry sample was kept in a desiccator filled with silica-gel desiccants before being used in further steps.

$$\text{Calculated EMImBF}_4\text{ in dry film} = \left(\frac{W_2}{W_1 + W_2}\right) \times 100\,, \tag{1}$$

where W_1 is the weight (in g) of CS and W_2 is the weight (in g) of $EMImBF_4$.

Table 1. Composition of CS solution for CS-TFEs.

Sample	Weight of CS [g]	Weight of water [g]	Weight of $EMImBF_4$ [g]	Calculated $EMImBF_4$ in dry film [wt%]
CS-BF_4-60	0.36	13.64	0.54	60
CS-BF_4-70			0.85	70
CS-BF_4-80			1.47	80

2.3. Characterizations

2.3.1. SEM

The structural morphology of each sample was observed using a scanning electron microscope (SEM; JSM6700, JEOL, Japan) at an accelerating voltage of 5 kV and a

magnification of 5,000.

2.3.2. FT–IR

The functional groups of each sample were characterized using a Fourier-transform infrared (FT-IR) spectrometer (FT/IR-4200, JASCO, Japan) via the KBr-pellet method in the wavenumber range of 400–4000 cm^{-1}.

2.3.3. TGA

The thermal decomposition of each sample was tested under a nitrogen atmosphere using a thermogravimetric analyzer (TGA; EXSTAR TG/DTA6200, SII, Japan). The sample was heated from 30°C to 550°C at a heating rate of 20°C/min.

2.3.4. Mechanical properties

The mechanical properties of each sample were determined in ambient conditions using a universal testing machine (STA-1150, A&D Company, Ltd., Japan) equipped with a 50-N load cell and operating at a constant speed of 10 mm/min. Before the analysis, the sample was cut to be 30 mm long and 5 mm wide and was mounted in tensile grips spaced 10 mm apart. The measurement was repeated more than 10 times. The tensile parameters of tensile strength and

elongation at break were determined from the stress–strain curves obtained from the force–distance data.

2.3.5. $EMImBF_4$ content

The amount of $EMImBF_4$ in an obtained sample was determined as follows. The sample was weighed, soaked in excess dichloromethane for 24 h to remove $EMImBF_4$, dried at 60°C for 24 h, and then weighed again. This procedure was repeated until the sample weighed the same before and after the $EMImBF_4$-removal step. A percentage of the total $EMImBF_4$ content was calculated according to Eq. (2).

$$\%\ \mathrm{EMImBF_4\ content} = \left(\frac{M_1 - M_2}{M_1} \right) \times 100\,, \tag{2}$$

where M_1 is the weight (in mg) of the $EMImBF_4$-bearing sample and M_2 is the constant weight (in mg) of the sample after removing $EMImBF_4$.

2.4. Fabrication of EDLC test cells and measurement of electrochemical properties

Each obtained TFE was cut into a 16-mm-diameter disk and soaked in $EMImBF_4$ under 0.3-Pa vacuum at room temperature for 48 h before being assembled in the EDLC test cell. The test cell was assembled by sandwiching the TFE between two carbon electrodes in a coin-cell (CR2032, stainless type, Hohsen Corporation, Japan) in an argon-filled glove box. In addition,

a test cell was assembled with liquid-phase $EMImBF_4$ with a cellulose separator (TF4035, Nippon Kodoshi Corporation, Japan) for comparison.

The symmetrical carbon electrodes were prepared by coating as follows. Activated carbon (YP-50F, specific surface area: 1500–1800 m^2/g, Kuraray Co., Ltd., Japan), acetylene black (HS-100, Denka Co., Ltd., Japan) as a conductive additive, 1.2 wt% sodium carboxymethyl cellulose (WS-C, DKS Co., Ltd., Japan) as a dispersant, and 48 wt% styrene–butadiene rubber (TRD2001, JSR Corporation, Japan) as a binder were mixed in DI water at a weight ratio of 90:5:3:2. The mixture was stirred until a homogenous slurry with a smooth surface was obtained. The obtained electrode slurry was coated on an aluminum current collector to produce a carbon electrode. The obtained carbon electrode was dried in an oven at 100°C for 10 h to eliminate the solvent and was then cut into a 12-mm-diameter disk before being used in the next steps.

The electrochemical properties of each EDLC test cell were determined in terms of its charge–discharge performance, discharge capacitance, and alternating-current (AC) impedance. The charge–discharge performance was measured using a battery charge/discharge apparatus (HJ1001 SM8, Hokuto Denko Corporation, Japan) at voltages of 0–2.5 V and various current densities. The discharge rate was estimated at discharge current densities between 2.5–100 mA/cm^2. The discharge capacitance of a single electrode in the symmetrical EDLC cell was determined using Eq. (3) [30, 31]:

$$C = \left(\frac{I \times t}{(V/2) \times W} \right), \quad (3)$$

where C is the discharge capacitance, I is the discharge current [A], t is the discharge time [s], V is the operating voltage, and W is the total mass of activated carbon in a single electrode [g].

The AC impedance was measured using a potentiogalvanostat (SI 1287, Solartron Analytical, UK) and a frequency-response analyzer (SI 1260, Solartron Analytical, UK) with an AC amplitude of 10 mV_{p-0} in the frequency range of 500 kHz–10 mHz. All electrochemical measurements were performed at 25°C.

3. Results and discussion

3.1. Preparation of CS-TEFs

CS is difficult to dissolve in commonly used solvents because it has strong hydrogen bonding and a combination of amorphous and crystalline regions. Therefore, for preparing the CS electrolytes (CS-gel) in the previous reports, CS powder was dissolved in aqueous acetic acid and the solution was cast to produce the films, later soaking it in IL [30–31]. In this study, we proposed a new method to prepare CS-TFE. CS was dissolved in a mixture of $EMImBF_4$ and water that could approximately control IL content in obtained product by one-pot synthesis, and $EMImBF_4$ acts as not only the solvent for the CS but also the charge carrier for the EDLCs.

3.2. Characterizations

3.2.1. SEM

SEM images of the surfaces and cross-sectional areas of the CS-TFE products are shown in Fig. 2. None of the surfaces show phase separation between the CS and $EMImBF_4$. By contrast, the surface morphology of the sample was influenced by the amount of $EMImBF_4$ in the dry film. CS-BF_4-60 (see Fig. 2(a)) had a grainy structure with unevenly distributed spots, suggesting that there was insufficient $EMImBF_4$ in the mixture solution to incorporate it into the CS matrix for complete dissolution. CS-BF_4-80 (see Fig. 2(c)) had a rough surface with a porous structure because of the low wt% of CS and high wt% of $EMImBF_4$ when the film was prepared. Moreover, the cross-sectional morphology of each sample was considered and showed that porosity was present throughout. The porosity size increased with the wt% of $EMImBF_4$ in the dry film, which could be related to the amount of CS and EMImBF4 in the mixture solution before the film was prepared.

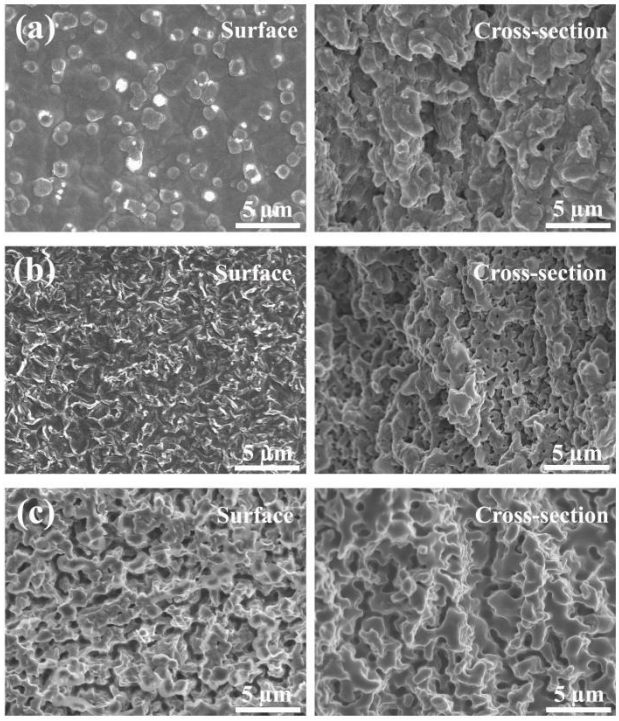

Fig. 2. SEM images of the surface and cross-sectional area of (a) CS-BF_4-60, (b) CS-BF_4-70, and (c) CS-BF_4-80.

3.2.2. FT-IR

The FT-IR spectra of $EMImBF_4$, CS powder, and CS-TFE products are shown in Fig. 3. The adsorption peak for the CS powder is similar to that of the CS-TFE products at characteristic peaks of CS as follows. The broad band around 3,450 cm^{-1} is due to the stretching vibrations of the $–NH_2$ and –OH groups. The broad bands at 2,920 and 2,860 cm^{-1} are due to the asymmetric stretching vibrations of C–H in the sugar residue. The peak around 1,690 cm^{-1} is due to the stretching of amide I. The peaks at 1,420, 1,380, and 1,320 cm^{-1} are due to CH_2 deformation, $–CH_3$ symmetric deformation, and amide III/CH_2 wagging, respectively [22, 56,

57]. By contrast, the characteristic peaks of $EMImBF_4$ were observed on the CS-TFE products only. The new peaks at 3,140 and 2,980 cm^{-1} are due to the aliphatic asymmetric and symmetric (C–H) stretching vibrations of the imidazolium ring. The new strong peak at 1,570 cm^{-1} is due to the C=C stretching vibration of the imidazolium ring. The increased adsorption peak at 1,169 cm^{-1} is due to the C–N stretching vibration of the imidazolium ring; in particular, the peak at 1,049 cm^{-1} corresponds to the asymmetric vibrations of B–F bond [58–60]. The FT-IR spectra confirm that $EMImBF_4$ was introduced effectively into the CS-TFE products.

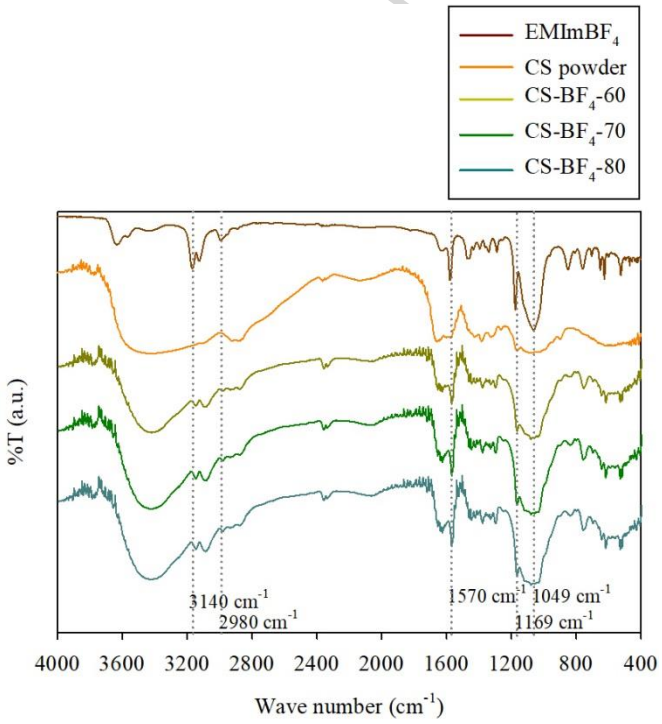

Fig. 3. FT-IR spectra of $EMImBF_4$, CS powder, and CS-TFE products.

3.2.3. TGA

The TGA and differential TGA (DTGA) curves of $EMImBF_4$, CS powder and CS-TFEs

products are shown in Figs. 4(a) and (b), respectively. The TGA thermograms show how the sample weight decreased during thermal decomposition, and the DTGA curves show clearly the maximum decomposition temperature at each step of thermal decomposition. The CS powder and all of the CS-TFE products lost weight at temperatures of approximately 30°C – 130°C because of the evaporation of volatile content. The CS powder showed only one thermal degradation step as obtained from the peak in the DTGA curve at 307°C corresponding to the chemical degradation and deacetylation of CS molecules [61]. By contrast, the CS-TFE products showed two distinctive thermal degradation stages. The first stage was observed at around 275°C, which is near the degradation temperature observed for the CS powder and could be due to CS decomposition. The second-stage degradation temperatures of CS-TFE products CS-BF_4-60, CS-BF_4-70, and CS-BF_4-80 were 421°C, 423°C, and 437°C, respectively. The degradation temperature increased with the $EMImBF_4$ content in the dry thin film, which is attributed mainly to the decomposition of $EMImBF_4$ [62, 63]; this can be seen also in the TGA and DTGA results for pure $EMImBF_4$. Therefore, it was shown that $EMImBF_4$ was incorporated successfully into the CS-TFEs.

Furthermore, all of the CS-TFE products showed high thermal stability. Therefore, this novel material has practical potential for use as electrolyte in EDLCs operating at high temperature.

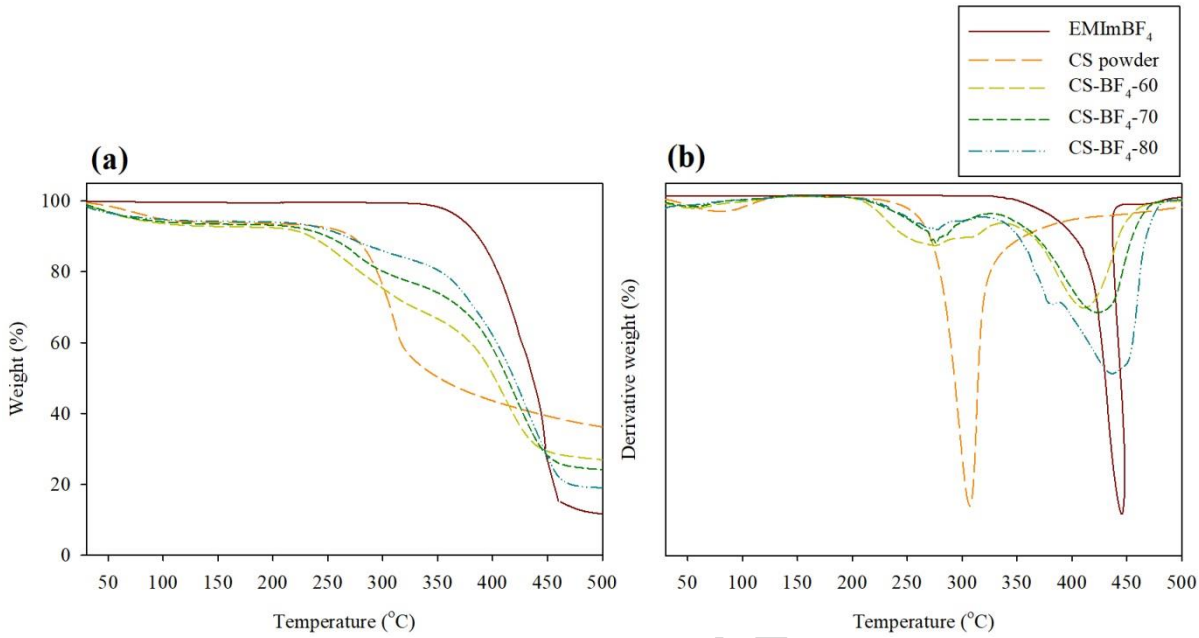

Fig. 4. (a) TGA and (b) DTGA curves of $EMImBF_4$, CS powder and CS-TFE products.

3.2.4. Mechanical properties

The tensile strength and elongation at break of the CS-TFE products are summarized in Table 2. Moreover, CS-gel from previous studies was replicated to compare their mechanical properties [30–31]. The tensile strength of a sample is the maximum tensile stress sustained during tensile testing. The tensile strength decreased with the wt% $EMImBF_4$ in the dry thin film because of the decrease of the CS mass and the porous structure of the sample. However, the lowest tensile strength of the thin-film samples (that of CS-BF_4-80) was significantly higher than those of all of CS-gel samples. The elongation at break of the CS-TFE products slightly improved compare to CS-gel from 33.44% to the range of 35.02%–36.94%. The experimental results suggest that the CS-TFE product from the new preparation method exhibited improved tensile properties compared to the CS-gel systems due to the different preparation method. The

viscosity of the cast solution of chitosan was higher in the present system than that in the CS-gel system, thus more dense film was prepared.

Table 2. Tensile strength and elongation at break of various samples.

Sample	Elongation at break [%]	Tensile strength [MPa]
CS-BF_4-60	36.67 ± 6.32	72.78 ± 7.13
CS-BF_4-70	36.97 ± 9.18	36.50 ± 5.34
CS-BF_4-80	35.02 ± 3.86	17.45 ± 3.18
CS-gel	33.44 ± 6.05	0.32 ± 0.06

3.2.5. $EMImBF_4$ content

The remaining amount of $EMImBF_4$ incorporated into the CS matrix from CS-TFE preparation process of CS-BF_4-60, CS-BF_4-70, and CS-BF_4-80 were 48.05%, 53.98%, and 70.21%, respectively. The $EMImBF_4$ content of the obtained samples increased with the wt% of $EMImBF_4$ in the mixture solution used for film preparation. This result proves that this new CS-TFE preparation method is able to approximately control IL content in obtained product by one-pot synthesis. Moreover, the obtained CS-TFE was soaked in $EMImBF_4$ solution before fabrication of the EDLC test cell. The $EMImBF_4$ content of CS-BF_4-60, CS-BF_4-70, and CS-BF_4-80 were increased to 51.1%, 58.0%, and 78.8%, respectively. The $EMImBF_4$ content of CS-BF_4-80 was significantly increased as compared with those of CS-BF_4-60 and CS-BF_4-70 because of the broad porous structure of the sample as obtained from the SEM observations: the film possibly adsorbed more $EMImBF_4$ after the sample was soaked in $EMImBF_4$.

3.3. Electrochemical properties

The obtained CS-TFEs or liquid-phase $EMImBF_4$ with a cellulose separator were assembled in EDLC test cells as electrolytes to test their electrochemical properties regarding charge–discharge performance, discharge capacitance, and Nyquist plots obtained by AC impedance measurements.

The charge–discharge curves of the EDLC test cells assembled with either liquid-phase $EMImBF_4$ or the obtained CS-TFEs are shown in Figs. 5(a), (b), and (c) for current densities of 2.5, 50, and 100 mA/cm^2, respectively. During the 2.5-mA/cm^2 charge–discharge measurements, all test cells showed a perfectly triangular shape that is a typical shape of the ideal EDLCs. In the charge–discharge curves measured at high current densities of 50 and 100 mA/cm^2, rapid voltage drops during switching (known as *IR* drops and indicated by arrow in Fig. 5(b)) occurred in all the test cells, showing a clearly larger *IR* drop with higher current density. However, the *IR* drop was reduced in the CS-TFEs with higher $EMImBF_4$ content. The CS-BF_4-60 and CS-BF_4-70 test cells showed larger *IR* drops than that of the test cell with liquid-phase $EMImBF_4$, whereas the CS-BF_4-80 test cell showed an *IR* drop that was comparable with that of the liquid-phase $EMImBF_4$ system; that may be because the ionic conductivity and internal resistance of the test cell were improved by increasing the $EMImBF_4$ content in the TFEs.

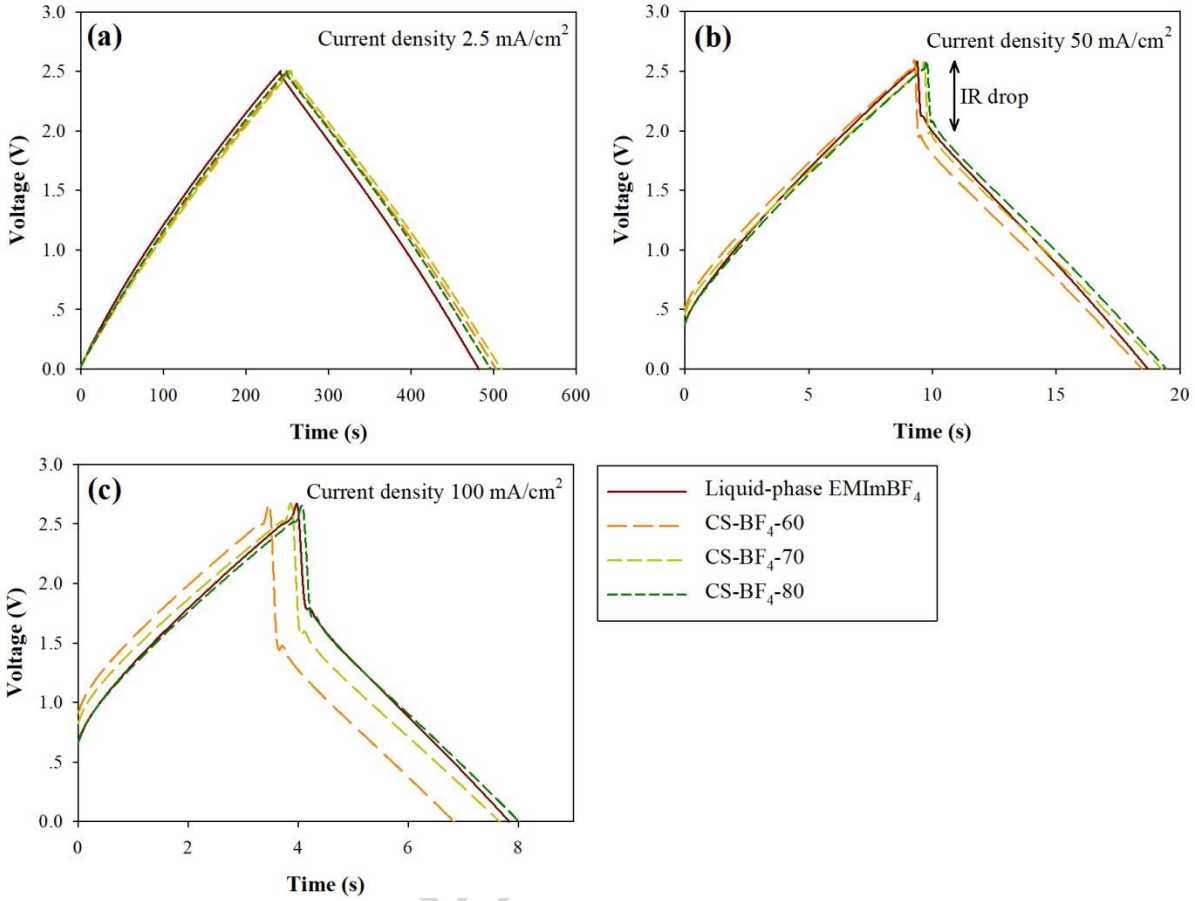

Fig. 5. Charge–discharge curves of the EDLC test cell assembled with liquid-phase $EMImBF_4$ or the obtained CS-TFEs at current densities of (a) 2.5, (b) 50, and (c) 100 mA/cm^2.

Furthermore, the discharge capacitances of the same EDLC test cells are shown in Fig. 6 as functions of the applied current density in the range 2.5–100 mA/cm^2. At low current density, the CS-BF_4-60 and CS-BF_4-70 test cells showed higher discharge capacitances compared to the liquid-phase $EMImBF_4$ test cell, becoming lower at higher current density. By contrast, the discharge capacitance of the CS-BF_4-80 test cell was higher compared to the liquid-phase

$EMImBF_4$ system over the entire range of current density. Moreover, the capacitance retentions of the test cells were calculated for 2.5–100 mA/cm^2. Those of the CS-BF_4-60, CS-BF_4-70, CS-BF_4-80, and liquid-phase $EMImBF_4$ test cells were 54%, 59%, 64%, and 64%, respectively, suggesting that the capacitance retention increased with the $EMImBF_4$ content in the CS-TFEs in the TFE system; the capacitance retention of the CS-BF_4-80 test cell was comparable to that of the liquid-phase $EMImBF_4$ system. Overall, the charge–discharge measurements show that CS-BF_4-80 is suitable and advantageous as an excellent electrolyte in EDLC applications.

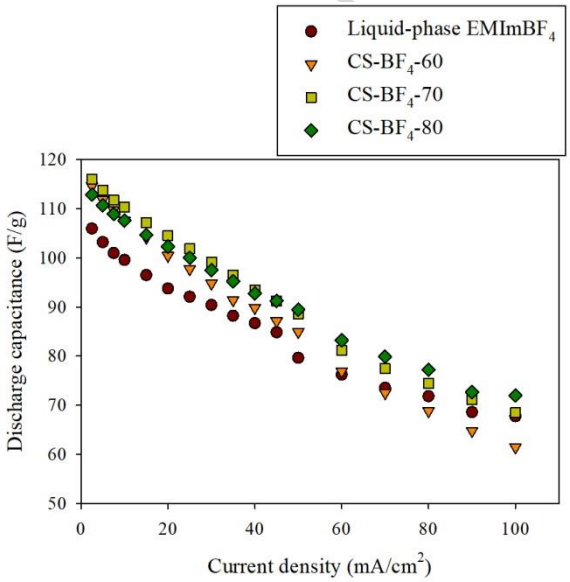

Fig. 6. Discharge capacitances of the EDLC test cell assembled with liquid-phase $EMImBF_4$ or the obtained CS-TFEs.

To investigate the electrochemical behavior at the electrode/electrolyte interface in detail,

AC impedance measurements were carried out on the EDLC test cells with various types of electrolyte. Nyquist plots obtained by AC impedance measurements on the EDLC test cells assembled with liquid-phase $EMImBF_4$ or the obtained CS-TFEs are shown in Fig. 7. All test cells showed a small semicircle at high frequencies (see inset of Fig. 7), followed by a transition to linearity at low frequencies, corresponding to a capacitive behavior [64]. Focusing on the semicircles, which represent the impedance of the parallel resistance and capacitance at the contact interface between activated carbon and electrolyte [65], the observed semicircles of the CS-BF_4-60 and CS-BF_4-70 test cells are larger than that of the test cell with liquid-phase $EMImBF_4$, whereas that of the test cell with the CS-BF_4-80 test cell is slightly smaller. This shows that the higher $EMImBF_4$ content in the TFEs improved the affinity between the activated carbon and TFE, thereby reducing the electronic-contact resistance in the activated-carbon electrode at the electrode/electrolyte interface. This may be attributed to the relatively high ionicity of ILs and the highly polarizable substituents of CS such as the R–NH_2 and R–OH groups [31].

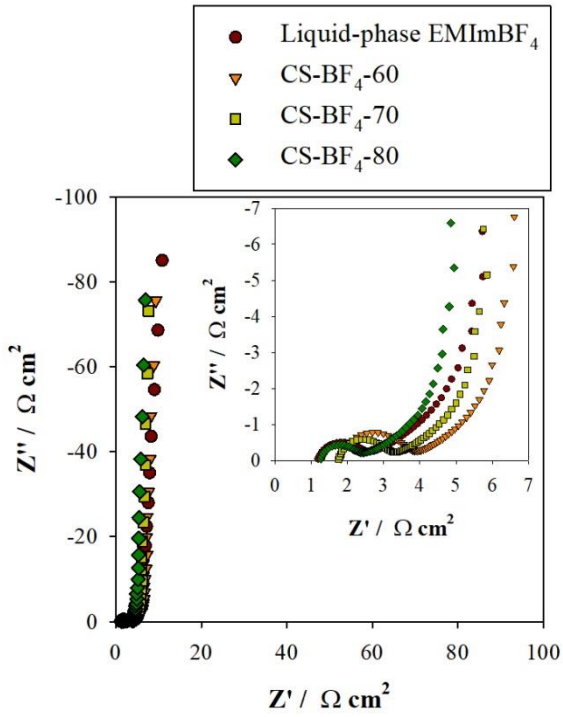

Fig. 7. Nyquist plots obtained by AC impedance measurements of the EDLC test cell assembled with the liquid-phase $EMImBF_4$ or the obtained CS-TFEs.

4. Conclusions

In this present work, a novel TFE as functionalized solid electrolyte was prepared from CS with $EMImBF_4$ via a new preparation method. CS powder was dissolved in a mixture of $EMImBF_4$ and DI water to produce CS-TFEs with different wt% of $EMImBF_4$ in the dry sample for the first time. In this system, $EMImBF_4$ plays important roles as a solvent and a charge carrier for EDLC applications. From structural characterizations, all of the obtained CS-TFEs from the new preparation method showed surfaces with no CS/$EMImBF_4$ phase separation, and the surface morphologies of the samples changed according to the dry-film wt% of $EMImBF_4$. The FT-IR spectra of the CS-TFE products showed peaks that were characteristic

of both CS and $EMImBF_4$, indicating that $EMImBF_4$ was incorporated efficiently into the CS matrix. The TGA and DTGA results revealed that the all of the CS-TFE products had high thermal stability. The results of tensile testing showed that the obtained samples from the new preparation method had significant higher tensile strength than that of the CS-gel from previous reports. Furthermore, the total $EMImBF_4$ content of the obtained samples (CS-BF_4-60, CS-BF_4-70, and CS-BF_4-80) is 51.1%, 58.0%, and 78.8%, respectively, and could be controlled by the preparation conditions of the CS solutions.

In addition, the obtained CS-TFEs were fabricated in EDLC test cells to measure their electrochemical properties in comparison with that of a test cell with a liquid-phase $EMImBF_4$ system. On testing the charge–discharge performance, the CS-BF_4-80 test cell exhibited an *IR* drop at high current density that was comparable to that of the liquid-phase $EMImBF_4$ test cell, and the former also showed a higher discharge capacitance over the current-density range of 2.5–100 mA/cm^2. Moreover, the results of the AC impedance measurements on the CS-BF_4-80 test cell showed decreased resistance at the electrode/electrolyte interface compared with the liquid-phase $EMImBF_4$ test cell. All of the results regarding electrochemical properties showed the CS-BF_4-80 TFE to be suitable and advantageous as an excellent solid electrolyte in the design of high-performance EDLCs, as well as for improving the safety of such devices.

Acknowledgements

This work was financially supported by Private University Research Branding Project, MEXT, 2016–2020 and in part by the Kansai University Outlay Support for Establishing Research Centers, 2016−2017. ‘Development and application of biocompatible polymer materials having sol-gel transition’.

References

[1] S. Kumagai, D. Tashima, Electrochemical performance of activated carbon prepared from rice husk in different type of non-aqueous electrolytes, Biomass Bioenergy 83 (2015) 216–223.

[2] A. Mundy, G.L. Plett, Reduced-order physics-based modeling and experimental parameter identification for non-Faradaic electrical double-layer capacitors, J. Energy Storage 7 (2016) 167–180.

[3] M. Tokita, N. Yoshimoto, K. Fujii, M. Morita, Degradation characteristics of electric double-layer capacitors consisting of high surface area carbon electrodes with organic electrolyte solutions, Electrochim. Acta 209 (2016) 210–218.

[4] M. Yamagata, K. Soeda, S. Yamazaki, M. Ishikawa, Charge-discharge behavior of electric double layer capacitor with alginate/ionic liquid gel electrolyte, J. Electrochem. Soc. 25 (35) (2010) 193–200.

[5] M. Yamagata, S. Ikebe, Y. Kasai, K. Soeda, M. Ishikawa, Dramatic improvements in

electric double-layer capacitors using polysaccharides. J. Electrochem. Soc. 50 (43) (2013) 27–36.

[6] K. Soeda, M. Yamagata, M. Ishikawa, Outstanding features of alginate-based gel electrolyte with ionic liquid for electric double layer capacitors, J. Power Sources 280 (2015) 565–572.

[7] N.N. Mobarak, N. Ramli, A. Ahmad, M.Y.A. Rahman, Chemical interaction and conductivity of carboxymethyl κ-carrageenan based green polymer electrolyte, Solid State Ionics 224 (2012) 51–57.

[8] S. Rudhziah, M.S.A. Rani, A. Ahmad, N.S. Mohamed, H. Kaddami, Potential of blend of kappa-carrageenan and cellulose derivatives for green polymer electrolyte application, Ind. Crops Prod. 72 (2015) 133–141.

[9] E. Raphael, C.O. Avellaneda, B. Manzolli, A. Pawlicka, Agar-based films for application as polymer electrolytes, Electrochim. Acta 55 (2010) 1455–1459.

[10] R. Leones, F. Sentanin, L.C. Rodrigues, I.M. Marrucho, J.M.S.S. Esperança, A. Pawlicka, M.M. Silva, eXPRESS polym. lett. 6 (12) (2012) 1007–1016.

[11] A.S.A. Khiar, A.K. Arof, Conductivity studies of starch-based polymer electrolytes, Ionics 16 (2010) 123–129.

[12] M. Kumar, T. Tiwari, N. Srivastava, Electrical transport behavior of bio-polymer electrolyte system: potato starch + ammonium iodide, Carbohydr. Polym. 88 (2012) 54–

60.

[13] M.F. Shukur, R. Ithnin, M.F.Z. Kadir, Electrical characterization of corn starch-LiOAc electrolytes and application in electrochemical double layer capacitor, Electrochim. Acta 136 (2014) 204–216.

[14] A.M.M. Ali, R.H.Y. Subban, H. Bahron, T. Winie, F. Latif, M.Z.A. Yahya, Ionics 14 (2008) 491–500.

[15] S.N. Mohamed, N.A. Johari, A.M.M. Ali, M.K. Harun, M.Z.A. Yahya, Electrochemical studies on epoxidized natural rubber-based gel polymer electrolytes for lithium-air cells, J. Power Sources 183 (2008) 351–354.

[16] R.K. Mishra, A. Anis, S. Mondal, M. Dutt, A.K. Banthia, Preparation and characterization of amidated pectin based polymer electrolyte membranes, Chin. J. Polym. Sci. 27 (5) (2009) 639–646.

[17] R. Ou, Y. Xie, X. Shen, F. Yuan, H. Wang, Q. Wang, Solid biopolymer electrolytes based on all-cellulose composite prepared by partially dissolving cellulosic fibers in the ionic liquid 1-butyl-3-methylimidazolium chloride, J. Mater. Sci. 47 (2012) 5978–5986.

[18] R. Alves, F. Sentanin, R.C. Sabadini, A. Pawlicka, M.M. Silva, Infiuence of cerium triflate and glycerol on electrochemical performance of chitosan electrolytes for electrochromic devices, Electrochim. Acta 217 (2016) 108–116.

[19] R. Leones, P.M. Reis, R.C. Sabadini, L.P. Ravaro, I.D.A. Silva, A.S.S. de Camargo, J.P.

Donoso, C.J. Magon, J.M.S.S. Esperança, A. Pawlicka, M.M. Silva, luminescent europium ionic liquid to improve the performance of chitosan polymer electrolytes, Electrochim. Acta 240 (2017) 474–485.

[20] R. Leones, R.C. Sabadini, J.M.S.S. Esperança, A. Pawlicka, Effect of storage time on the ionic conductivity of chitosan-solid polymer electrolytes incorporating cyano-based ionic liquids, Electrochim. Acta 232 (2017) 22–29.

[21] R. Jayakumar, H. Nagahama, T. Furuike, H. Tamura, Synthesis of phosphorylated chitosan by novel method and its characterization, Int. J. Biol. Macromol. 42 (2008) 335–339.

[22] A. Anitha, V.V.D. Rani, R. Krishna, V. Sreeja, N. Selvamurugan, S.V. Nair, H. Tamura, R. Jayakumar, Synthesis, characterization, cytotoxicity and antibacterial studies of chitosan, *O*-carboxymethyl and *N*,*O*-carboxymethyl chitosan nanoparticles, Carbohydr. Polym. 78 (2009) 672–677.

[23] K. Madhumathi, K.T. Shalumon, V.V.D. Rani, H. Tamura, T. Furuike, N. Selvamurugan, S.V. Nair, R. Jayakumar, Wet chemical synthesis of chitosan hydrogel–hydroxyapatite composite membranes for tissue engineering applications, Int. J. Biol. Macromol. 45 (2009) 12–15.

[24] H. Nagahama, H. Maeda, T. Kashiki, R. Jayakumar, T. Furuike, H. Tamura, Preparation and characterization of novel chitosan/gelatin membranes using chitosan hydrogel,

Carbohydr. Polym. 76 (2009) 255–260.

[25] Y. Saito, V. Luchnikov, A. Inaba, K. Tamura, Self-scrolling ability of differentially acetylated chitosan film, Carbohydr. Polym. 109 (2014) 44–48.

[26] T. Furuike, D. Komoto, H. Hashimoto, H. Tamura, Preparation of chitosan hydrogel and its solubility in organic acids, Int. J. Biol. Macromol. 104 (2017) 1620–1625.

[27] R. Jayakumar, N. Selvamurugan, S.V. Nair, S. Tokura, H. Tamura, Preparative methods of phosphorylated chitin and chitosan–An overview, Int. J. Biol. Macromol. 43 (2008) 221–225.

[28] R. Jayakumar, M. Prabaharan, S.V. Nair, H. Tamura, Novel chitin and chitosan nanofibers in biomedical applications, Biotechnol. Adv. 28 (2010) 142–150.

[29] R. Jayakumar, M. Prabaharan, P.T. Sudheesh Kumar, S.V. Nair, H. Tamura, Biomaterials based on chitin and chitosan in wound dressing applications, Biotechnol. Adv. 29 (2011) 322–337.

[30] M. Yamagata, K. Soeda, S. Ikebe, S. Yamazaki, M. Ishikawa, Polysaccharide-based gel electrolyte containing hydrophobic ionic liquids for electric double-layer capacitors, J. Electrochem. Soc. 41 (2012) 25–34.

[31] M. Yamagata, K. Soeda, S. Ikebe, S. Yamazaki, M. Ishikawa, Chitosan-based gel electrolyte containing an ionic liquid for high-performance nonaqueous supercapacitors, Electrochim. Acta 100 (2013) 275–280.

[32] K. Soeda, M. Yamagata, S. Yamazaki, M. Ishikawa, Application of chitosan-based gel electrolytes with ionic liquids for high-performance and safe electric double layer capacitors, Electrochemistry 81 (10) (2013) 867–872.

[33] J. Chupp, A. Shellikeri, G. Palui, J. Chatterjee, Chitosan-based gel film electrolytes containing ionic liquid and lithium salt for energy storage applications, J. Appl. Polym. Sci. 132 (26) 42143.

[34] X. Mu, X. Yang, D. Zhang, C. Liu, Theoretical study of the reaction of chitosan monomer with 2,3-epoxypropyl-trimethyl quaternary ammonium chloride catalyzed by an imidazolium-based ionic liquid, Carbohydr. Polym. 146 (2016) 46–51.

[35] W. Wang, J. Zhu, X. Wang, Y. Huang, Y. Wang, Dissolution behavior of chitin in ionic liquids, J. Macromol. Sci., Part B 49 (3) (2010) 528–541.

[36] K. Wilpiszewska, T. Spychaj, Ionic liquids: Media for starch dissolution, plasticization and modification, Carbohydr. Polym. 86 (2011) 424–428.

[37] A. Lewandowski, M. Galiński, Carbon–ionic liquid double-layer capacitor, J. Phys. Chem. Solids 65 (2004) 281–286.

[38] Z. Zhou, M. Takeda, M. Ue, New hydrophobic ionic liquid based on perfluoroalkyltrifluoroborate anions, J. Fluorine Chem. 125 (2004) 471–476.

[39] T. Sato, G. Masuda, K. Takagi, Electrochemical properties of novel ionic liquids for electric double layer capacitor applications, Electrochim. Acta 49 (2004) 3603–3611.

[40] K. Yuyama, G. Masuda, H. Yoshida, T. Sato, Ionic liquids containing the tetrafluoroborate anion have the best performance and stability for electric double layer capacitor applications, J. Power Sources 162 (2006) 1401–1408.

[41] C.O. Ania, J. Pernak, F. Stefaniak, E. Raymundo-Piñero, F. Béguin, Solvent-free ionic liquids as in situ probes for assessing the effect of ion size on the performance of electrical double layer capacitors, Carbon 44 (2006) 3126–3130.

[42] N. Handa, T. Sugimoto, M. Yamagata, M. Kikuta, M. Kono, M. Ishikawa, A neat ionic liquid electrolyte based on FSI anion for electric double layer capacitor, J. Power Sources 185 (2008) 1585–1588.

[43] D.M. Phillips, L.F. Drummy, D.G. Conrady, D.M. Fox, R.R. Naik, M.O. Stone, P.C. Trulove, H.C. De Long, R.A. Mantz, Dissolution and regeneration of bombyx mori silk fibroin using ionic liquids, J. Am. Chem. Soc. 126 (2004) 14350–14351.

[44] O.A.E. Seoud, A. Koschella, L.C. Fidale, S. Dorn, T. Heinze, Applications of ionic liquids in carbohydrate chemistry: A window of opportunities, Biomacromolecules 8 (9) (2007) 2629–2647.

[45] I. Kilpeläinen, H. Xie, A. King, M. Granstrom, S. Heikkinen, D.S. Argyropoulos, Dissolution of wood in ionic liquids, J. Agric. Food Chem. 55 (2007) 9142–9148.

[46] R.P. Swatloski, S.K. Spear, J.D. Holbrey, R.D. Rogers, Dissolution of cellose with ionic liquids, J. Am. Chem. Soc. 124 (2002) 4974–4975.

[47] M.E. Zakrzewska, E. Bogel-Łukasik, R. Bogel-Łukasik, Solubility of carbohydrates in ionic liquids, Energy Fuels 24 (2010) 737–745.

[48] B. Meenatchi, V. Renuga, A. Manikandan, Cellulose dissolution and regeneration using various imidazolium based protic ionic liquids, J. Mol. Liq. 238 (2017) 582–588.

[49] H. Xie, S. Zhang, S. Lib, Chitin and chitosan dissolved in ionic liquids as reversible sorbents of CO_2, Green Chem. 8 (2006) 630–633.

[50] W. Xiao, Q. Chen, Y. Wu, T. Wu, L. Dai, Dissolution and blending of chitosan using 1,3-dimethylimidazolium chloride and 1-H-3-methylimidazolium chloride binary ionic liquid solvent, Carbohydr. Polym. 83 (2011) 233–238.

[51] S.S. Silva, J.F. Mano, R.L. Reis, Ionic liquids in the processing and chemical modification of chitin and chitosan for biomedical applications, Green Chem. 19 (2017) 1208–1220.

[52] G. Santos-López, W. Argüelles-Monal, E. Carvajal-Millan, Y.L. López-Franco, M.T. Recillas-Mota, J. Lizardi-Mendoza, Aerogels from chitosan solutions in ionic liquids, Polym. 9 (2017) 722.

[53] Q. Chen, A. Xu, Z. Li, J. Wang, S. Zhang, Influence of anionic structure on the dissolution of chitosan in 1-butyl-3-methylimidazolium-based ionic liquids, Green Chem. 13 (2011) 3446–3452.

[54] X. Sun, Q. Tian, Z. Xue, Y. Zhang, T. Mu, The dissolution behaviour of chitosan in

acetate based ionic liquids and their interactions: from experimental evidence to density functional theory analysis, RSC Adv. 4 (2014) 30282–30291.

[55] Q. Tian, S. Liu, X. Sun, H. Sun, Z. Xue, T. Mu, Theoretical studies on the dissolution of chitosan in 1-butyl-3-methylimidazolium acetate ionic liquid, Carbohydr. Res. 408 (2015) 107–113.

[56] S. Kumari, S.H.K. Annamareddy, S. Abanti, P.K. Rath, Physicochemical properties and characterization of chitosansynthesized from fish scales, crab and shrimp shells, Int. J. Biol. Macromol. 104 (2017) 1697–1705.

[57] R.A. Mauricio-Sánchez, R. Salazar, J.G. Luna-Bárcenas, A. Mendoza-Galván, FTIR spectroscopy studies on the spontaneous neutralization of chitosan acetate films by moisture conditioning, Vib. Spectrosc 94 (2018) 1–6.

[58] Y. Wang, X. Gao, R. Wang, H. Liu, C. Yang, Y. Xiong, Effect of functionalized montmorillonite addition on the thermal properties and ionic conductivity of PVDF–PEG polymer electrolyte, React. Funct. Polym. 68 (2008) 1170–1177.

[59] S. Ambika, M. Sundrarajan, [EMIM] BF_4 ionic liquid-mediated synthesis of TiO_2 nanoparticles using *Vitex negundo Linn* extract and its antibacterial activity, J. Mol. Liq. 221 (2016) 986–992.

[60] T. Romann, O. Oll, P. Pikma, H. Tamme, E. Lust, Surface chemistry of carbon electrodes in 1-ethyl-3-methylimidazolium tetrafluoroborate ionic liquid – anin situ infrared study,

Electrochim. Acta 125 (2014) 183–190.

[61] C.Y. Soon, Y.B. Tee, C.H. Tan, A.T. Rosnita, A. Khalina, Extraction and physicochemical characterization of chitin and chitosan from *Zophobas morio* larvae in varying sodium hydroxide concentration, Int. J. Biol. Macromol. 108 (2018) 135–142.

[62] G. Min, T. Yim, H.Y. Lee, D.H. Huh, E. Lee, J. Mun, S.M. Oh, Y.G. Kim, Synthesis and properties of ionic liquids: Imidazolium tetrafluoroborates with unsaturated side chains, Bull. Korean Chem. Soc. 27 (6) (2006) 847–852.

[63] Y. Cao, T. Mu, Comprehensive investigation on the thermal stability of 66 ionic liquids by thermogravimetric analysis, Ind. Eng. Chem. Res. 53 (2014) 8651–8664.

[64] C. Yang, S. Hsu, W. Chien, All solid-state electric double-layer capacitors based on alkaline polyvinyl alcohol polymer electrolytes, J. Power Sources 152 (2005) 303–310.

[65] A. Lewandowski, A. Świderska, Electrochemical capacitors with polymer electrolytes based on ionic liquids, Solid State Ionics 161 (2003) 243–249.